Inorg. Chem. **2002**, *41*, 1412–1420

Pyrazolyl-Bridged Iridium Dimers. 18.[1] Influence of Metal–Metal Bonding on the Geometry of Diiridium(II) Adducts and Hydrido-diiridium Complexes Formed from the Diiridium(I) Prototype $[Ir(\mu\text{-pz})(PPh_3)(CO)]_2$ (pzH = Pyrazole) by Dihydrogen Addition or Protonation

Ron D. Brost, Gordon W. Bushnell, Daryll G. Harrison, and Stephen R. Stobart*

Department of Chemistry, University of Victoria, Victoria, British Columbia, Canada V8W 2Y2

Received April 26, 2001

Slow uptake of molecular dihydrogen by the diiridium(I) prototype $[Ir(\mu\text{-pz})(PPh_3)(CO)]_2$ (**1**: pzH = pyrazole) is accompanied by formation of a 1,2-dihydrido-diiridium(II) adduct $[IrH(\mu\text{-pz})(PPh_3)(CO)]_2$ (**2**), for which an X-ray crystal structure determination reveals that (unlike in **1**) the PPh_3 ligands are axial, with the hydrides occupying trans coequatorial positions across the Ir–Ir bond (2.672 Å). Reaction with CCl_4 effects hydride replacement in **2**, affording the monohydride $Ir_2H(Cl)(\mu\text{-pz})_2(PPh_3)_2(CO)_2$ (**3**) in which Ir–Ir = 2.683 Å. At one metal center, H is equatorial and PPh_3 is axial, while at the other, Cl is axial as is found in the symmetrically substituted product $[Ir(\mu\text{-pz})(PPh_3)(CO)Cl]_2$ (**4**) (Ir–Ir = 2.754 Å) that is formed by action of CCl_4 on **1**. Treatment of **1** with I_2 yields the diiodo analogue **5** of **4**, which reacts with $LiAlH_4$ to afford the isomorph $Ir_2H(I)(\mu\text{-pz})_2(PPh_3)_2(CO)_2$ (**6**) of **3** (Ir–Ir = 2.684 Å). Protonation (using HBF_4) of **1** results in formation of the binuclear cation $Ir_2H(\mu\text{-pz})_2(PPh_3)_2(CO)_2^+$ (**7**: BF_4^- salt), which shows definitive evidence (from NMR) for a terminally bound hydride in solution (CH_2Cl_2 or THF), but **7** crystallizes as an axially symmetric unit in which Ir–Ir = 2.834 Å. Reaction of **7** with water or wet methanol leads to isolation of the cationic diiridium(III) products $[Ir_2H_2(\mu\text{-OX})(\mu\text{-pz})_2(PPh_3)_2(CO)_2]BF_4$ (**8**, X = H; **9**, X = Me).

Introduction

Binuclear transition-metal complexes in which a folded bridging framework holds coordinatively unsaturated d^8 sites in proximity to each other[1,2] are characterized by a nominal bond order of zero between the two metal atoms. This results from orbital overlap and occupancy that can be represented in a simplified way as $(d\sigma)^2(d\sigma^*)^2$. It follows that reductive activation of an external substrate by interaction with the formally antibonding HOMO ($d\sigma^*$), which initiates a two-center oxidative addition reaction,[2] will be accompanied by the development of a metal−metal bond between the two adjacent centers. Not only is this a physically demonstrable change, but it offers a rationalization in terms of simple electron counting for the diamagnetism of products that are formally the result of a unit increase in the oxidation state at each metal center. It is in this domain that the d^7 +2 state has emerged[3] as an important conjunction in the chemistry of iridium. Thus, in particular, it has been shown that $d^7{}_2$ complexes ($Ir^{II}-Ir^{II}$) can function as stable termini to oxidative steps using binuclear $d^8{}_2$ prototypes;[4] can exist in equilibrium with the latter;[5] or can be accessed reductively from oxidized $d^6{}_2$ analogues.[6] It is striking, therefore, that although concerted addition of dihydrogen to a mononuclear metal center (including, conspicuously, d^8 Ir^I) is a familiar event,[7] only a handful of reports exist of iridium dimers

* Corresponding author. E-mail: stobartz@uvvm.uvic.ca.

(1) Part 17: Arthurs, M. A.; Bickerton, J.; Stobart, S. R.; Wang, J. *Organometallics* **1998**, *17*, 2743.
(2) Schmidbaur, H.; Franke, R. *Inorg. Chim. Acta* **1975**, *13*, 85. Lewis, N. S.; Mann, K. R.; Gordon, J. G. H.; Gray, H. B. *J. Am. Chem. Soc.* **1976**, *98*, 7461. Che, C. M.; Schaefer, W. P.; Gray, H. B.; Dickson, M. K.; Stein, F.; Roundhill, D. M. *J. Am. Chem. Soc.* **1982**, *104*, 4253. Marshall, J. L.; Stobart, S. R.; Gray, H. B. *J. Am. Chem. Soc.* **1984**, *106*, 3027. Fackler, J. P., Jr.; Murray, H. H.; Basil, J. D. *Organometallics* **1984**, *3*, 821. Ling, S. S. M.; Jobe, I. R.; Manojlovic-Muir, L.; Muir, K. W.; Puddephatt, R. J. *Organometallics* **1985**, *4*, 1198.
(3) Coleman, A. W.; Eadie, D. T.; Stobart, S. R.; Zaworotko, M. J.; Atwood, J. L. *J. Am. Chem. Soc.* **1982**, *104*, 922. Cotton, F. A.; Laheurta, P.; Sanau, M.; Schwotzer, W. *J. Am. Chem. Soc.* **1985**, *107*, 8284.
(4) Bushnell, G. W.; Fjeldsted, D. O. K.; Stobart, S. R.; Wang, J. *Organometallics* **1996**, *15*, 3785.
(5) Brost, R. D.; Fjeldsted, D. O. K.; Stobart, S. R. *J. Chem. Soc., Chem. Commun.* **1989**, 488.
(6) Bailey, J. A.; Grundy, S. L.; Stobart, S. R. *Organometallics* **1990**, *9*, 536.

10.1021/ic010448g CCC: $22.00
Published on Web 02/21/2002

reacting similarly.[8−11] Direct uptake of molecular hydrogen by any neutral homobinuclear transition-metal complex has in fact remained distinguished by its rarity,[12] although such addition[13] to a mixed-valence (Ir^0-Ir^{II}, i.e., d^9-d^7) diiridium core, together with the demonstration[14] that parahydrogen-induced polarization (PHIP) can be used to characterize its stereochemical profile, are two very recent and exciting developments in this context.

In our preliminary report[9] describing facile two-fragment, two-center oxidative addition as a characteristic of the prototypal iridium(I) dimer $[Ir(\mu\text{-pz})(PPh_3)(CO)]_2$ (**1**: pzH = pyrazole), we indicated that as well as reacting in such a manner with[15] dihalogens and alkyl halides, dihydrogen also adds to **1** to afford a 1,2-dihydrido-diiridium(II) adduct $[IrH(\mu\text{-pz})(PPh_3)(CO)]_2$ (**2**). In the interim, this has remained one of the very few[8−14] examples of such behavior: it is not observed for analogues of **1**, including[16] $[Ir(\mu\text{-pz})(CO)_2]_2$ and[17] $[Ir(\mu\text{-pz})(COD)]_2$ (COD = cycloocta-1,5-diene), nor is it paralleled in an extensive study by Oro and co-workers[18] of the reactivity of other dimers related to **1**. We describe below the verification of the structure of **2** by using X-ray diffraction as well as by its derivatization to a crystallographically characterized monohydrido analogue $Ir_2H(Cl)(\mu\text{-pz})_2(PPh_3)_2(CO)_2$ (**3**), together with the formation of the iodo analogue of **3** by monosubstitution of the diiodo adduct $[IrI(\mu\text{-pz})(PPh_3)(CO)]_2$ of **1**. A cationic diiridium(II) product of protonation of **1**, $[Ir_2H(\mu\text{-pz})_2(PPh_3)_2(CO)_2]BF_4$, has also been isolated. The bimetallic core of the cation adopts an axially symmetric structure in the crystalline state, with the single hydride ligand assigned to a bridging position across an iridium−iridium contact that is contracted to within bonding range (2.834 Å). This symmetrical structure clearly does not persist in solution, however, because NMR spectroscopy reveals differential coupling (ABX array) of a high-field proton to nonequivalent phosphorus centers, an observation that is consistent only with terminal attachment of H to a unique Ir atom. Although we have yet to investigate the reactivity of this protonated complex with dihydrogen, we have found that it is susceptible to further oxidation. In particular, it is extremely sensitive to hydrolysis, undergoing oxidative addition of water, a process that remains[19] extremely rare either at mononuclear or binuclear centers.

Experimental Section

A. General Considerations. Synthetic methodology and instruments used for spectroscopic measurements have been referred to extensively in earlier papers in this series.[1,15,16] The isotopically labeled reagents ^{13}CO and triphenylphosphine-d_{15} were used as received (Aldrich) or obtained by using published procedures.[20] Conductivities were measured in acetone solution using a Copenhagen conductivity meter with a CDC324 small-volume electrode (nominal cell constant = 0.316 cm) and calibration versus $NHEt_3$-Cl.

B. Synthesis of Neutral Diiridium Complexes. i. $[Ir(\mu\text{-pz})(PPh_3)(CO)]_2$ (1). This complex was synthesized as described[15] earlier as an orange-red microcrystalline solid that deteriorates slowly in air. An isotopomer $[Ir(\mu\text{-pz})(PPh_3)(^{13}CO)]_2$ (**1a**) was prepared as follows: a solution of the precursor $[Ir(\mu\text{-pz})(COD)]_2$ (100 mg, 0.14 mmol) in tetrahydrofuran (20 mL) was frozen at −196° C, evacuated, and then exposed to gaseous ^{13}CO (30 mL at 1.0 atm, 1.34 mmol). On warming to ambient temperature, followed by rapid stirring, the initially red solution turned intensely yellow within 25 min. Addition of triphenylphosphine (73 mg, 0.28 mmol) led to immediate gas evolution and a color change to bright orange; the product was recovered[15] in 91% yield. An isotopomer of **1a**, $[Ir(\mu\text{-pz})(PPh_3\text{-}d_{15})(CO)]_2$ (**1b**), may be obtained (>95% atomic purity) by addition of labeled phosphine to **1a** after the carbonylation step.

ii. $[IrH(\mu\text{-pz})(PPh_3)(CO)]_2$ (2). A slurry of **1** (1.12 g, 1.02 mmol) in diethyl ether (35 mL) was formed in a glass liner fitted to a Parr Instrument Co. model 316 high-pressure reactor, which was then purged and pressurized to 1000 psig with dihydrogen gas. After 24 h at 35° C,the supernatant was decanted, and the solid residue composed of a mixture of small colorless crystals and white microcrystalline material (0.82 g, 0.070 mmol, 73%) was recovered. A crystal suitable for X-ray diffraction was collected by hand-sorting. Anal. Calcd for $C_{44}H_{38}Ir_2N_4O_2P_2$: C, 48.0; H, 3.5; N, 5.1. Found: C, 47.6; H, 3.6; N, 5.3. Stirring solutions of compound **1** in benzene or toluene in an atmosphere of dihydrogen led to very slow deposition (over 48 h) of **2** as a fine, pale yellow powder.

iii. $Ir_2H(Cl)(\mu\text{-pz})_2(PPh_3)_2(CO)_2$ (3). Carbon tetrachloride (5 mL) was added to a solution of **2** (100 mg, 0.09 mmol) in dichloromethane (25 mL). While the mixture was stirred at 20° C, it turned from colorless to yellow. After 18 h, the solvent was removed, leaving a yellow solid that was recrystallized from dichloromethane/hexanes to yield air-stable, X-ray quality material (80 mg, 0.07 mmol, 78%). Anal. Calcd for $C_{44}H_{37}ClIr_2N_4O_2P_2$: C, 46.5; H, 3.3; N, 4.9. Found: C, 46.2; H, 3.3; N, 4.9.

iv. $[IrCl(\mu\text{-pz})(PPh_3)(CO)]_2$ (4). Carbon tetrachloride (3 mL) was stirred with **1** (75 mg, 0.07 mmol) in diethyl ether (20 mL) for 1 h, during which time the solution changed color from bright orange to yellow. Removal of the solvent left an oil. Redissolution

(7) James, B. R. *Homogeneous Hydrogenation*; Wiley & Sons: New York, 1973. See also James, B. R. In *Comprehensive Organometallic Chemistry*; Wilkinson, G., Stone, F. G. S., Abel, E. W., Eds.; Pergamon Press: New York, 1982; Vol. 8, Chapter 51. Collman, J. P.; Hegadus, L. S.; Norton, J. R.; Finke, R. G. *Principles and Applications of Organotransition Metal Chemistry*; University Science Books: Mill Valley, CA, 1987; Chapter 10.

(8) Bonnet, J. J.; Thorez, A.; Maisonnat, A.; Galy, J.; Poilblanc, R. *J. Am. Chem. Soc.* **1979**, *101*, 5940.

(9) Beveridge, K. A.; Bushnell, G. W.; Dixon, K. R.; Eadie, D. T.; Stobart, S. R.; Atwood, J. L.; Zaworotko, M. J. *J. Am. Chem. Soc.* **1982**, *104*, 920.

(10) Sutherland, B. R.; Cowie, M. *Organometallics* **1985**, *4*, 1801. Vaartstra, B. A.; Cowie, M. *Inorg. Chem.* **1989**, *28*, 3138.

(11) Schnabel, R. C.; Roddick, D. M. *Organometallics* **1996**, *15*, 3550.

(12) Jiménez, M. V.; Sola, E.; Martínez, A. P.; Lahoz, F. J.; Oro, L. A. *Organometallics* **1999**, *18*, 1125.

(13) Heyduk, A. F.; Nocera, D. G. *J. Am. Chem. Soc.* **2000**, *122*, 9145.

(14) Oldham, S. M.; Houlis, J. F.; Sleigh, C. J.; Duckett, S. B.; Eisenberg, R. *Organometallics* **2000**, *19*, 2985.

(15) Atwood, J. L.; Beveridge, K. A.; Bushnell, G. W.; Dixon, K. R.; Eadie, D. T.; Stobart, S. R.; Zaworotko, M. J. *Inorg. Chem.* **1984**, *23*, 4050.

(16) Beveridge, K. A.; Bushnell, G. W.; Stobart, S. R.; Atwood, J. L.; Zaworotko, M. J. *Organometallics* **1983**, *2*, 1447.

(17) Harrison, D. G.; Stobart, S. R. *J. Chem. Soc., Chem. Commun.* **1986**, 285.

(18) Tejel, C.; Ciriano, M. A.; López, J. A.; Lahoz, F. J.; Oro, L. A. *Organometallics* **1997**, *16*, 4718 and references therein.

(19) Burn, M. J.; Fickes, M. G.; Hartwig, J. F.; Hollander, F. J.; Bergman, R. G. *J. Am. Chem. Soc.* **1993**, *115*, 5875. Yoon, M.; Tyler, D. R. *J. Chem. Soc., Chem. Commun.* **1997**, 639. Kaplan, A. W.; Bergman, R. G. *Organometallics* **1997**, *16*, 1106. Tani, K.; Iseki, A.; Yamagata, T. *Angew. Chem., Int. Ed.* **1998**, *37*, 3381. Dorta, R.; Togni, A. *Organometallics* **1998**, *17*, 3423. Stobart, S. R.; Zhou, X.; Cea-Olivares, R.; Toscano, A. *Organometallics* **2001**, *20*, 4766.

(20) Bianco, V. D.; Doronzo, S. *Inorg. Synth.* **1976**, *16*, 18.

in dichloromethane (3 mL) followed by careful addition of a layer of hexanes led to slow crystallization of the pale yellow, air-stable product (60 mg, 0.05 mmol, 75%). Anal. Calcd for $C_{44}H_{36}Cl_2Ir_2N_4O_2P_2$: C, 45.2; H, 3.1; N, 4.8. Found: C, 45.5; H, 3.2; N, 5.0.

v. [IrI(μ-pz)(PPh$_3$)(CO)]$_2$ (5). Crystalline diiodine (94 mg, 0.74 mmol) was dissolved in tetrahydrofuran (3 mL) and then added drop-by-drop to a slurry of **1** (0.41 g, 0.37 mmol) in diethyl ether (20 mL). A bright yellow precipitate was immediately deposited; after 15 min, the precipitate was allowed to settle, and then the supernatant was removed. The solid residue was washed thoroughly with hexanes and then dried under vacuum to yield the product as a light yellow powder (0.49 g, 0.36 mmol, 97%). Anal. Calcd for $C_{44}H_{36}I_2Ir_2N_4O_2P_2$: C, 39.1; H, 2.7; N, 4.1. Found: C, 38.7; H, 2.5; N, 4.0.

vi. Ir$_2$H(I)(μ-pz)$_2$(PPh$_3$)$_2$(CO)$_2$ (6). An excess of solid lithium aluminum hydride (50 mg, 1.3 mmol) was carefully added to a slurry of **5** (0.25 g, 0.19 mmol) in diethyl ether (20 mL). After agitation for 30 min, a pale yellow precipitate was allowed to settle. Removal of the solvent, washing the precipitate with ether, and then redissolution of the precipitate in dichloromethane (30 mL) was followed by filtration through a Celite plug and then concentration to a 5 mL volume. Thereafter, the product was deposited slowly as pale yellow, air-stable needles (50 mg, 0.04 mmol, 22%). Anal. Calcd for $C_{44}H_{37}IIr_2N_4O_2P_2$: C, 43.1; H, 3.0; N, 4.6. Found: C, 43.2; H, 2.9; N, 4.5.

C. Synthesis of Cationic Diiridium Complexes. i. [Ir$_2$H(μ-pz)$_2$(PPh$_3$)$_2$(CO)$_2$]BF$_4$ (7). To a solution of **1** (180 mg, 0.16 mmol) in diethyl ether (60 mL) was added tetrafluoroboric acid diethyl etherate (5 drops, excess). Precipitation of a bright yellow solid occurred immediately; after 20 min, this solid was recovered by removal of the supernatant, followed by repeated washing of the residue with diethyl ether. After the product was dried under vacuum, it was collected as a bright yellow powder (178 mg, 0.15 mmol, 94%). Anal. Calcd for $C_{44}H_{37}BF_4Ir_2N_4O_2P_2$: C, 44.52; H, 3.14; N, 4.72. Found: C, 44.48; H, 3.07; N, 4.66. Conductivity (in acetone): 99 Ω^{-1} cm^2 mol^{-1}. Crystals suitable for X-ray diffraction were grown at $-30°$ C from a dichloromethane solution under a layer of hexanes. In another experiment, addition of tetrafluoroboric acid diethyl etherate (10 drops, excess) to a rapidly agitated slurry of **1** (0.75 g, 0.68 mmol) in diethyl ether (40 mL) led to instant precipitation of a pale yellow solid. This solid was allowed to settle, and after 10 min, it was collected as a dry, air-stable, pale yellow powder (0.8 g, 0.68 mmol, 99%). Found: C, 44.3; H, 3.1; N, 4.9. Addition of diethyl ether to a saturated solution of this material in tetrahydrofuran resulted in the slow deposition of crystals suitable for X-ray diffraction.

ii. [Ir$_2$H$_2$(μ-OH)(μ-pz)$_2$(PPh$_3$)$_2$(CO)$_2$]BF$_4$ (8). Compound **7** (100 mg, 0.09 mmol) was dissolved in dichloromethane (20 mL), water (3 drops) was added, and then the solution was stirred for 6 h. Volatile material was pumped away, and then the yellow oily residue was washed with hexanes (3 × 10 mL). Drying overnight in vacuo afforded a light yellow, air-stable solid (93 mg, 0.08 mmol, 93%). Anal. Calcd for $C_{44}H_{39}BF_4Ir_2N_4O_3P_2$: C, 43.2; H, 3.1; N, 4.6. Found: C, 43.7; H, 3.2; N, 4.3. Conductivity (in acetone): 100 Ω^{-1} cm^2 mol^{-1}. Use of dideuterium oxide instead of water yielded an isotopomer of **8**, **8**-$^2H_2$.

iii. [Ir$_2$H$_2$(μ-OMe)(μ-pz)$_2$(PPh$_3$)$_2$(CO)$_2$]BF$_4$ (9). Compound **7** (80 mg, 0.07 mmol) was stirred in methanol (10 mL) for 12 h. The slightly turbid solution was evaporated under vacuum, leaving a light yellow oil. This oil was washed with hexanes and then dried in vacuo to give a yellow powder (65 mg). The product was shown by NMR spectroscopy to contain ca. 30% of **8**, which could not be removed by fractional crystallization.

iv. [Ir$_2$(μ-I)(μ-pz)$_2$(PPh$_3$)$_2$(CO)$_2$]BF$_4$ (10). When silver tetrafluoroborate (43 mg, 0.22 mmol) in acetone (5 mL) was added dropwise to a stirred solution of **5** (150 mg, 0.11 mmol) in acetone (20 mL), the color of the solution faded in 60 s, and a yellow solid precipitated. Filtration through Celite followed by removal of acetone left a yellow oil that was washed with ether (2 × 10 mL) and then with hexanes (10 mL). This procedure afforded the product as a deep yellow, air-sensitive powder. Anal. Calcd for $C_{44}H_{36}BF_4IIr_2N_4O_2P_2$: C, 40.2; H, 2.7; N, 4.3. Found: C, 40.2; H, 2.4; N, 4.3. Conductivity (in acetone): 108 Ω^{-1} cm^2 mol^{-1}.

v. [Ir$_2$H(μ-I)(μ-pz)$_2$(I)(PPh$_3$)$_2$(CO)$_2$]BF$_4$ (11). Slow addition of tetrafluoroboric acid diethyl etherate (5 drops, excess) to a stirred solution of **5** (200 mg, 0.15 mmol) in dichloromethane (20 mL) led to a color change from yellow to deep red within 15 s. After 10 min, the volume was reduced to 5 mL, and ether (15 mL) was added to precipitate a solid that was separated and then washed with ether. Drying in vacuo left an air-stable, brick-red product (196 mg, 0.14 mmol, 92%). Anal. Calcd for $C_{44}H_{37}BF_4I_2Ir_2N_4O_2P_2$: C, 36.7; H, 2.6; N, 3.9. Found: C, 36.4; H, 2.4; N, 3.6. Conductivity (in acetone): 101 Ω^{-1} cm^2 mol^{-1}.

D. Reaction of 1 with Trifluoroacetic Acid. To **1** (0.37 g, 0.34 mmol) in diethyl ether (20 mL) was added trifluoroacetic acid (10 drops, excess) with stirring (1 h). Evaporation of the clear yellow solution to dryness followed by washing with hexanes (3 × 10 mL) left behind the majority of a solid white product, **12** (0.32 g, 0.23 mmol, 71%). Anal. Calcd for $C_{48}H_{38}F_6Ir_2N_4O_6P_2$: C, 43.4; H, 2.9; N, 4.2. Found: C, 43.2; H, 2.7; N, 4.3. Conductivity (in acetone): 0.7 Ω^{-1} cm^2 mol^{-1}.

E. X-ray Crystallography. All procedures conformed to those adopted earlier.[4,15,16] Additional details, including metric parameters, are included in the Supporting Information. Crystal data for compounds **2**−**4**, **6**, and **7** are collected in Table 1. For structures **2**−**4** and **6**, phenyl carbon atoms as well as hydrogen atoms were refined isotropically, as is discussed further in the Supporting Information.

Results

Uptake of gaseous hydrogen by orange-yellow solutions of the diriidium(I) complex [Ir(μ-pz)(PPh$_3$)(CO)]$_2$ (**1**) is very slow at ambient pressure. At 70 bar, however, this process accounts for complete conversion within 24 h to an almost colorless solid, [IrH(μ-pz)(PPh$_3$)(CO)]$_2$ (**2**), that was characterized analytically as a product of dihydrogen addition. Further insight into the nature of this compound is provided by the spectroscopic data collected in Table 2. IR spectra (using KBr pellets) show a very strong band attributable to ν_{CO}, which is shifted to higher wavenumbers compared to the corresponding band of **1**. A weak, broad feature above 2150 cm^{-1} is also tentatively assigned to ν_{IrH}, although here as well as in related hydrides (see Table 2) identification of the band center was somewhat arbitrary, and its position is likely to be influenced by vibrational mixing with ν_{CO}.[21] In the ^{1}H NMR (see Table 2) spectrum, three resonances of equal intensity for hydrogens on the bridging-pz ligands correspond to[15] symmetrical disubstitution along the Ir$_2$ axis, and a single high-field proton signal centered at -16.15 ppm shows triplet structure, $J = 7.6$ Hz. The latter is indicative of "virtual coupling" to two chemically equivalent P nuclei that are strongly coupled to each other, suggesting a diaxial

(21) Poilblanc, R. *Inorg. Chim. Acta* **1982**, *62*, 75. Guilmet, E.; Maisonnat, A.; Poilblanc, R. *Organometallics* **1983**, *2*, 1123.

Table 1. Crystal Data[a]

compound	**2**	**3**	**4**	**6**	**7**
	$Ir_2P_2O_2N_4C_{44}H_{38}$	$Ir_2ClP_2O_2N_4C_{44}H_{37}$	$Ir_2Cl_2P_2O_2N_4C_{44}H_{38}$	$Ir_2IP_2O_2N_4C_{44}H_{37}$	$Ir_2P_2F_4O_2N_4C_{44}BH_{37}$
fw (g/mol)	1101.2	1135.6	1170.1	1227.1	1187.0
F(000) (e)	4241.0	4249.0	967.0	4284.0	2284.0
space group	*I*2/*a* (No. 15)	*Pbca*	$P\bar{1}$ (No. 2)	*Pbca*	*C*2/*c*
a (Å)	33.065(6)	16.748(4)	11.002(1)	16.772(4)	10.303(5)
b (Å)	13.657(8)	20.027(5)	13.035(2)	20.513(6)	23.372(9)
c (Å)	19.357(8)	24.462(4)	15.281(2)	24.287(6)	17.931(8)
α (deg)	90	90	110.42(1)	90	90
β (deg)	109.20(4)	90	93.47(2)	90	96.85(7)
γ (deg)	90	90	93.83(1)	90	90
cell volume	8255(7)	8205(3)	2041(3)	8356(3)	4287(3)
Z	8	8	2	8	4
D(calc) (g cm^{-3})	1.77	1.84	1.91	1.95	1.84
cryst size (mm)	0.15 × 0.21 × 0.06	0.1 × 0.1 × 0.05	0.1 × 0.1 × 0.05	0.3 × 0.1 × 0.03	0.2 × 0.2 × 0.2
abs coeff (cm^{-1})	65.36	66.43	67.43	71.90	63.12
data quadrant (2θ)	$\pm h,+k,+l < 451$	$+h,+k,+l < 401$	$+h, \pm k, \pm l < 401$	$+h,+k,+l < 451$	$\pm h,+k,+l < 50$
no. of unique reflections	3843	3837	3429	5472	3773
no. of reflections in L.S.	1461	2732	2381	3866	2871
no. of parameters.	162	246	255	246	286
GOF	1.6557	2.1104	1.8718	1.6914	1.3460
R	0.0956	0.0741	0.0688	0.0652	0.0409
R_w	0.1001	0.0921	0.0850	0.0786	0.0543
max shift/esd	0.0005	0.007	0.0005	0.0005	0.0005

[a] $\lambda_{radiation}$ = 0.71069 Å, *T* = 295 K, weak reflection cutoff $I/\sigma(I) < 2.5$.

relationship between the phosphine ligands in a structure derived from that of **1** by entry of H at an equatorial site at each Ir center. Accordingly, the $^{31}P\{^1H\}$ NMR spectrum consists of a singlet (Table 2); there is no NMR evidence for the existence of more than one geometrical isomer in solution. The availability of small, thin crystals allowed a crystallographic structure determination to be performed on **2**, although only to *R*(final) > 9%. Connectivity is clearly established, however, and the contraction of the Ir_2 separation to within bonding range as well as the presence of an axial phosphine ligand at each Ir center are each unambiguously recognizable. The carbonyl ligands occupy distal coordination sites that are related by C_2 rotation (i.e., the two CO ligands are trans to one another across the Ir−Ir bond) rather than by a proximal relationship (i.e., with the two CO ligands cis to one another, as is found in the thiolato-bridged analogue described[8,21] by Poilblanc et al.). Such a structure is fully consistent with all the spectroscopic data and shows that addition of H_2 to **1** produces a 1,2-dihydrido geometry in which the H atoms are trans to one another across the Ir_2 vector (see Scheme 1).

On boiling in CCl_4, substitution of only one H on Ir in **2** by Cl takes place, yielding the first of two isomorphous monohydrido dimers related to **2** that have also been identified crystallographically. The product **3** exhibits (Table 2) two ^{31}P NMR signals and six bridging-^1H resonances, which is consistent only with a binuclear structure that is unsymmetrically substituted along the Ir_2 axis. A high-field ^1H resonance (δ −16.72) appears as a doublet of doublets, with coupling constants of 15 and 1.5 Hz that are typical of $^2J_{cis}$ to P_A and ^3J to P_B across an Ir−Ir bond. The geometry suggested by these data (Scheme 1) has been verified by a single-crystal X-ray structure determination (see below). The hydride ligand at one metal center has been replaced by chloride. Entry of the chloride at an axial site relocates one PPh_3 to a position that is equivalent to that found in **1**.

Scheme 1

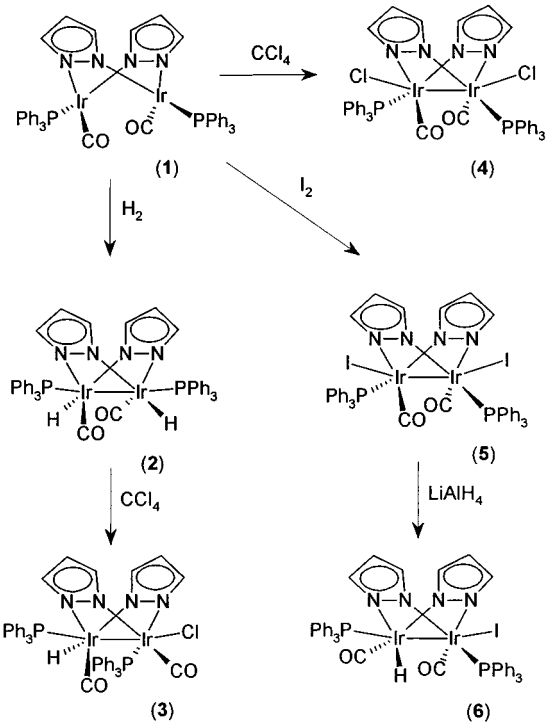

Refluxing unoxidized **1** in CCl_4 or allowing it to react under mild conditions with I_2 leads to an archetypal adduct geometry of $[IrX(\mu\text{-pz})(PPh_3)(CO)]_2$ (**4**, X = Cl; **5**, X = I) through occupation of both axial sites at diiridium(II) by halide. Additional reaction of **5** with $LiAlH_4$ generates **6**, which is an analogue of **3**. Thus, **6** has spectroscopic properties that closely resemble those of **3** (Table 2), although the ^3J coupling to P_B is not resolved. We used X-ray diffraction to confirm the unsymmetrical binuclear configuration of **6**, whose crystals are isomorphous with those of **3**, resulting from replacement of a single axial iodide by an equatorial hydride (Scheme 1).

Table 2. Spectroscopic Data

compound	IR[a] (cm^{-1})	^{1}H NMR[b] μ-pz	^{1}H NMR[b] other[c]	^{31}P NMR
1[d]	1962 (s)	7.58 (2H), 6.52 (2H), 5.84 (2H)		−123.4
2	2169 (w)[e], 2156 (m)[e], 2002 (s), 1976 (s)	6.60 (2H), 6.39 (2H), 5.65 (2H)	−16.15 (2H)	−143.2
3	2230 (m)[e], 2080 (s), 2060 (s)	7.73 (1H), 6.81 (1H), 6.58 (1H), 6.07 (1H), 5.93 (1H), 5.49 (1H)	−16.72 (1H)	−155.7, −137.0[f]
4	2034 (s), 2013 (sh)	7.67 (2H), 6.31 (2H), 5.58 (2H)		−147.2
5	2028 (s), 2012 (s)	7.88 (2H), 6.54 (2H), 5.54 (2H)		−148.9
6	2200 (m)[e], 2020 (s), 1990 (s)	7.80 (1H), 6.71 (1H), 6.53 (1H), 5.98 (1H), 5.83 (1H), 5.40 (1H)	−16.67 (1H)	−151.1, −138.5
7	2220 (w)[e], 2055 (s), 20l6 (s)	8.05 (1H), 7.89 (1H), 6.90 (1H), 6.75 (1H), 6.01 (1H), 5.73 (1H)	−25.50 (1H)	−135.5, −133.2
8[g]	2200 (w)[e,h], 2185[e], 2057 (s, br)	7.69 (2H), 6.81 (2H), 5.91 (2H)	−17.95 (2H)	−140.2
9	n.m.[i]	7.83 (2H), 6.37 (2H), 5.83 (2H)	3.57 (3H)[j], −19.00 (2H)	−144.1
10	2040 (s), 2020 (s)	6.69 (2H), 5.84 (2H)[k]		−140.5
11	2190 (m)[e], 2065 (s), 2010 (sh)	8.43 (1H), 7.85 (1H), 6.68 (2H), 5.96 (1H), 5.77 (1H)	−13.93 (1H)	−162.3, −144.4
12[l]	2256 (w)[e], 2238 (w)[e], 2059 (s)	7.60 (2H), 6.64 (2H), 5.87 (2H)	−17.24 (2H)	−143.0

[a] ν_{CO} (KBr) unless otherwise indicated. [b] δ (CD_2Cl_2 soln). [c] δ (Ir*H*) unless otherwise indicated. PPh_3 resonances observed in δ 7.60−7.10 range (30H). [d] Reference 25. [e] ν_{IrH}. [f] $CDCl_3$ soln. [g] ^{1}H signal attributable to δ (O*H*) not observed. [h] ν_{IrD} at 1580 (w). [i] n.m. = not measured. [j] δ (OCH_3). [k] Third μ-pz resonance obscured by PPh_3 hydrogens. [l] δ ^{19}F = −75.3.

Because **3** and **6** are putatively hydrogen halide adducts of the parent **1**, the effect of bubbling gaseous, anhydrous HX (X = Cl, Br, or I) into solutions of **1** was also examined, although stoichiometric addition of these reagents was not. Monitoring by NMR indicated the prompt formation of mononuclear products,[22] with no evidence that any binuclear adduct intermediates formed. By contrast, unoxidized **1** was found to react rapidly with HBF_4. Analytical data supported the incorporation of 1 mol equiv of HBF_4 into **1** to yield a bright yellow product, **7**, that precipitated from diethyl ether and behaved in acetone as a 1:1 electrolyte. The IR spectrum of solid **7** (in KBr) showed a weak band at 2220 cm^{-1} that was attributable to terminal Ir−H stretching, as well as ν_{CO} at 2050 and 2010 cm^{-1} and ν_{BF} at 1050 cm^{-1}. Dissolution of **7** in dichloromethane led to a ^{1}H NMR spectrum in which five of the six pz hydrogens are distinguishable (Table 2) from one another, while a conspicuous high-field resonance at −25.5 (dd) ppm was split by couplings of J = 15.4 and 4.2 Hz, which are attributable to cis $^2J_{HIrP}$ and $^3J_{HIrIrP}$, respectively. The ^{31}P NMR spectrum showed singlets at −133 and −136 ppm. To our surprise, quite different parameters were recorded for **7** in THF-d_8 (Table 2). Six bridging-hydrogen environments were again resolved, but at high-field a signal centered at −15.7 ppm appeared to be a doublet with J = 17.3 Hz, and the two ^{31}P shifts were more widely separated (−135, −142 ppm). Using dichloromethane and tetrahydrofuran, crystals that differed in their cell dimensions were grown independently; however, on investigation of both materials crystallographically, the data from the product obtained from dichloromethane (which led to the more accurate of the two independent structure determinations) led to the conclusion that these materials have rigorous two-fold symmetry, with hydrogens that are tentatively located at bridging rather than at terminal sites.

Traces of water in NMR solvents led to progressive conversion of the cation in **7** to a hydrido species that is characterized by a new high-field resonance at −17.9 ppm with $^2J_{cis}$ (to P) = 16.5 Hz. Addition of water accelerated the formation of this product, **8**, which showed only three NMR signals attributable to bridging-pz protons and a single ^{31}P resonance. A solution of **7** in methanol generated a very similar ^{1}H NMR spectrum for a new complex, **9** (Table 2), with a doublet at −19.0 ppm ($^2J_{cis}$ = 15.8) and an additional singlet at 3.57 ppm (OCH_3). Product **9** was found to be contaminated with **8**. The spectroscopic, analytical, and conductivity data are consistent with the formulation of **8** as a diiridium(III) cation (Scheme 2) that has a terminal H at each metal center and a bridging-OH group that is replaced by OMe in the methoxy-bridged analogue **9**. Compound **7** also changed color under an atmosphere of H_2S gas, and new high-field hydrogen resonances were observed, but no single major product could be separated.

Access to binuclear cationic fluoroborates from the diiododiiridium(II) adduct **5** was also explored. Thus, treatment of neutral **5** with $AgBF_4$ afforded a deep yellow powder that, on the basis of NMR spectra (Table 2) as well as microanalytical and conductivity data, was formulated as the symmetrical diiridium(II) cation **10** (Scheme 2). After abstraction of one iodide ligand (as AgI), this product is presumably formed by a rearrangement in which the second ligand undergoes terminal-bridge relocation. In accordance with this conclusion, further reaction of **10** with sodium hydride led metathetically to the formation of the protonated analogue **7**, which was formed as a mixture with its H_2O adduct **8**. Neutral **5** also reacted immediately with HBF_4, yielding a brick-red solid that, when analyzed, indicated 1:1 addition; in solution, this product showed two rather widely separated ^{31}P signals (Table 2) and a doublet ^{1}H NMR signal at −13.9 ppm ($^2J_{cis}$ = 14.7) that was accompanied by six

(22) Bailey, J. A.; Grundy, S. L.; Stobart, S. R. *Inorg. Chim. Acta* **1996**, *243*, 47.

Scheme 2

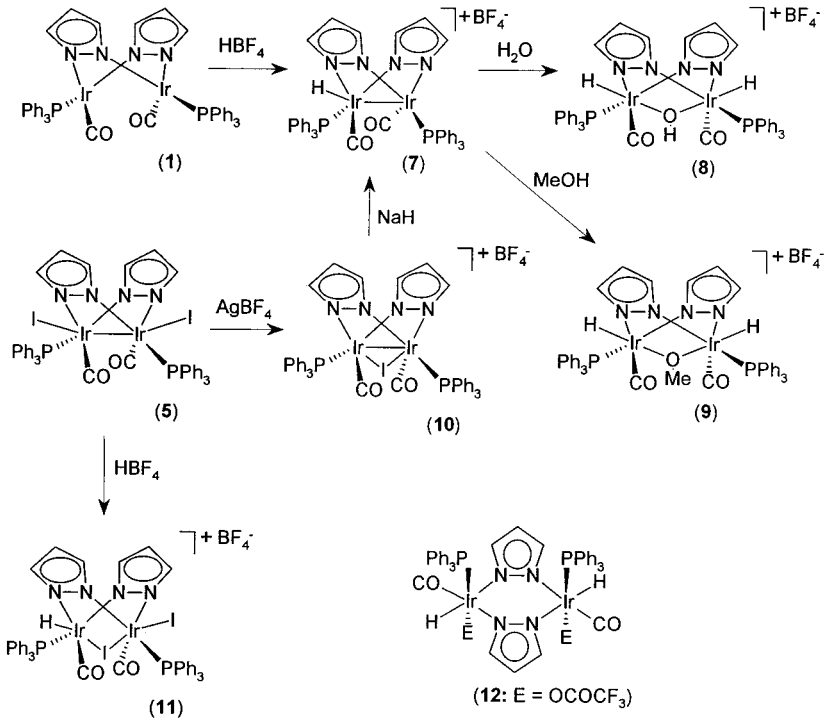

distinguishable resonances attributable to pz hydrogens. These data are consistent with an unsymmetrically[15] substituted binuclear cation **11**, in which, as in **10**, an iodide rather than a hydride occupies the endo bridging site (Scheme 2). Finally, addition to the prototype **1** of anhydrous trifluoroacetic acid was investigated, with the expectation that a cationic complex related to **7**−**9** or **11** would be formed. Instead, a colorless, neutral product was isolated and was shown by microanalytical data to contain one carboxylato group per Ir atom. The IR spectrum contained weak, very high-energy features attributable to ν_{IrH} (2256, 2238 cm^{-1}), bands near 1670 cm^{-1} assigned to CF_3CO_2, and typically strong bands assigned to ν_{CO}. A polyisotopic parent peak in the FAB mass spectrum corresponded to the binuclear ion $[Ir_2H_2(pz)_2(PPh_3)_2(CO)_2(CF_3CO_2)_2]^+$. Singlet resonances were observed in both the ^{31}P and ^{19}F NMR spectra, which are indicative of a highly symmetrical configuration. Accordingly, in the ^1H spectrum, three (rather than six, q.v.) pz hydrogen resonances were evident and were accompanied by a high-field feature (−17.2 ppm, $^2J_{cis}$ = 18.1) that accounted for two hydrogens upon signal integration. All these observations are consistent with the oxidation of precursor **1** to a formal diiridium(III) state in a complex possessing a structure unrelated to any of those of **2**−**11**, but rather one based on an edge-sharing bioctahedral arrangement, **12**.

Discussion

In the crystalline state, **1** adopts[15] classic folded binuclear geometry in which the pyrazolyl-bridged metallacyclic unit acts as a hinge between the square coordination environments that surround the adjacent d^8 metal centers. The phosphine ligands occupy in-plane (equatorial) sites that are trans to one another across the Ir_2 axis so that the molecule is atropisomeric.[4] Dihydrogen addition to this dimer affords[9] **2**, the X-ray structure of which establishes the molecular geometry that is shown in Figure 1. The phosphines have been twisted into the axial sites, leaving a conspicuous equatorial vacancy at each metal atom that corresponds to the position of a nonlocated hydride ligand. Both the latter and the two carbonyl ligands are trans to one another across the metal−metal vector, thus preserving in **2** the C_2 symmetry[4,15] of unoxidized **1**; however, the Ir−Ir distance is contracted to within bonding range (2.672 Å, see Table 3), as it should be for a diamagnetic diiridium(II) adduct.[4] These features correspond in all respects to those reported by Poilblanc et al.[8,21,23] for the only direct analogue $[IrH(\mu\text{-}SBu^t)(CO)\{P(OMe)_3\}]_2$, except that in the latter, the nonlocated hydrogen atoms are located cis coequatorial (C_s symmetry) to one another. Either type of coequatorial site-

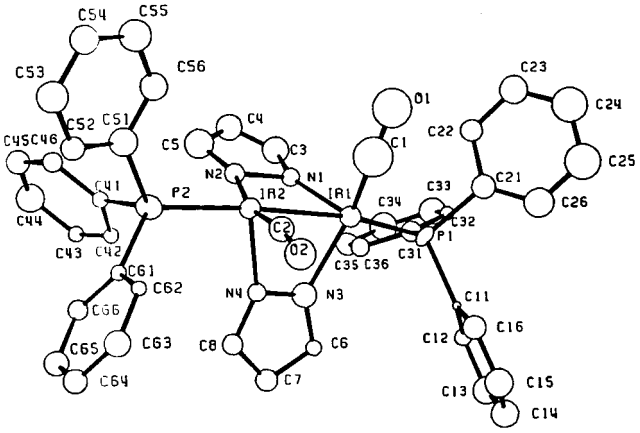

Figure 1. Molecular geometry of compound **2**.

Table 3. Selected Interatomic Distances and Angles for Compounds **2**−**4**, **6**, and **7**

compound	**2**		**3**		**4**		**6**		**7**	
				Interatomic Distances (Å)						
Ir(2)−Ir(1)	2.672(4)	Ir(2)−Ir(1)	2.683(2)	Ir(2)−Ir(1)	2.754(2)	Ir(2)−Ir(1)	2.684(1)	Ir(1′)−Ir(1)	2.834(1)
P(1)−Ir(1)	2.34(2)	Cl−Ir(1)	2.485(7)	Cl(2)−Ir(1)	2.448(8)	I−Ir(1)	2.782(2)	P(1)−Ir(1)	2.302(2)
P(2)−Ir(2)	2.33(2)	P(1)−Ir(1)	2.328(8)	Cl(1)−Ir(2)	2.410(9)	P(1)−Ir(1)	2.318(5)	N(1)−Ir(1)	2.069(6)
N(1)−Ir(1)	2.11(5)	P(2)−Ir(2)	2.328(8)	P(2)−Ir(1)	2.325(8)	P(2)−Ir(2)	2.326(5)	N(2′)−Ir(1)	2.053(6)
N(2)−Ir(2)	2.01(5)	N(1)−Ir(1)	2.07(3)	P(1)−Ir(2)	2.320(9)	N(1)−Ir(1)	2.10(2)	C(1)−Ir(1)	1.844(11)
N(3)−Ir(1)	2.19(5)	N(2)−Ir(2)	2.20(3)	N(1)−Ir(1)	2.06(3)	N(2)−Ir(2)	2.16(2)		
N(4)−Ir(2)	2.20(4)	N(3)−Ir(2)	2.05(2)	N(2)−Ir(2)	2.05(2)	N(3)−Ir(2)	2.05(2)		
C(1)−Ir(1)	1.79(2)[a]	N(4)−Ir(1)	2.05(2)	N(3)−Ir(1)	2.07(3)	N(4)−Ir(1)	2.10(2)		
C(2)−Ir(2)	1.76(2)[a]	C(7)−Ir(2)	1.78(3)	N(4)−Ir(2)	2.05(2)	C(7)−Ir(2)	1.74(2)		
		C(8)−Ir(1)	1.71(3)	C(7)−Ir(2)	1.83(3)	C(8)−Ir(1)	1.78(2)		
				C(8)−Ir(1)	1.75(4)				
				Interatomic Angles (deg)					
P(1)−Ir(1)−Ir(2)	169.1(5)	Cl−Ir(1)−Ir(2)	156.8(2)	Cl(2)−Ir(1)−Ir(2)	151.3(2)	I−Ir(1)−Ir(2)	158.2(1)	N(1)−Ir(1)−P(1)	174.9(2)
P(2)−Ir(2)−Ir(1)	166.2(5)	P(2)−Ir(2)−Ir(1)	167.0(2)	Cl(1)−Ir(2)−Ir(1)	150.8(2)	P(2)−Ir(2)−Ir(1)	168.1(1)	N(2′)−Ir(1)−C(1)	175.3(3)
C(1)−Ir(1)−N(3)	164.6(14)	C(8)−Ir(1)−N(4)	169.8(11)	N(3)−Ir(1)−P(2)	172.3((8)	C(8)−Ir(1)−N(4)	169.1(7)	C(1)−Ir(1)−P(1)	92.3(3)
C(2)−Ir(2)−N(2)	165.(2)	C(7)−Ir(2)−N(3)	170.7(11)	N(2)−Ir(2)−P(1)	176.4(6)	C(7)−Ir(2)−N(3)	168.1(8)	C(1)−Ir(1)−N(1)	92.7(3)
N(3)−Ir(1)−P(1)	95.2(15)	N(1)−Ir(1)−P(1)	171.5(6)	N(1)−Ir(1)−C(8)	169.2(13)	N(1)−Ir(1)−P(1)	170.1(4)	N(2′)−Ir(1)−P(1)	92.1(3)
N(2)−Ir(2)−P(2)	93.1(14)	N(4)−Ir(1)−Cl	88.7(6)	N(4)−Ir(2)−C(7)	173.5(12)	N(4)−Ir(1)−I	92.7(4)	N(2′)−Ir(1)−N(1)	82.8(3)
N(3)−Ir(1)−Ir(2)	74.5(14)	N(3)−Ir(2)−P(2)	93.1(7)	N(1)−Ir(1)−P(2)	92.0(8)	N(3)−Ir(2)−P(2)	96.5(5)	Ir(1′)−Ir(1)−N(2′)	69.6(3)
N(2)−Ir(2)−Ir(1)	76.3(14)	C(8)−Ir(1)−Cl	98.5(9)	N(4)−Ir(2)−P(1)	93.3(7)	C(8)−Ir(1)−I	95.0(6)	Ir(1′)−Ir(1)−N(1)	68.3(3)
C(1)−Ir(1)−Ir(2)	91.(2)	C(7)−Ir(2)−P(2)	95.7(8)	C(8)−Ir(1)−P(2)	97.5(11)	C(7)−Ir(2)−P(2)	95.3(7)	Ir(1′)−Ir(1)−P(1)	110.6(3)
C(2)−Ir(2)−Ir(1)	93.(2)	C(8)−Ir(1)−Ir(2)	98.4(9)	C(7)−Ir(2)−P(1)	86.4(10)	C(8)−Ir(1)−Ir(2)	99.0(6)	Ir(1′)−Ir(1)−C(1)	107.6(3)
C(1)−Ir(1)−P(1)	100.(2)	C(7)−Ir(2)−Ir(1)	97.0(8)	N(3)−Ir(1)−C(8)	89.7(14)	C(7)−Ir(2)−Ir(1)	95.9(7)		
C(2)−Ir(2)−P(2)	99.(2)	N(4)−Ir(1)−Ir(2)	72.8(6)	N(2)−Ir(2)−C(7)	97.1(12)	N(4)−Ir(1)−Ir(2)	71.5(4)		
N(1)−Ir(1)−P(1)	104.2(13)	N(3)−Ir(2)−Ir(1)	74.4(7)	N(3)−Ir(1)−N(1)	81.1(11)	N(3)−Ir(2)−Ir(1)	72.5(4)		
N(4)−Ir(2)−P(2)	101.5(12)	N(1)−Ir(1)−Ir(2)	72.6(7)	N(4)−Ir(2)−N(2)	83.3(9)	N(1)−Ir(1)−Ir(2)	72.3(4)		
N(1)−Ir(1)−N(3)	86.(2)	N(2)−Ir(2)−Ir(1)	71.9(6)	P(2)−Ir(1)−Cl(2)	86.5(3)	N(2)−Ir(2)−Ir(1)	72.0(4)		
N(4)−Ir(2)−N(2)	88.(2)	N(4)−Ir(1)−N(1)	83.0(8)	P(1)−Ir(2)−Cl(1)	89.6(3)	N(4)−Ir(1)−N(1)	82.7(6)		
N(1)−Ir(1)−Ir(2)	72.0(12)	N(3)−Ir(2)−N(2)	85.9(8)	C(8)−Ir(1)−Cl(2)	97.8(11)	N(3)−Ir(2)−N(2)	86.8(6)		
N(4)−Ir(2)−Ir(1)	69.8(10)	N(1)−Ir(1)−Cl	91.8(7)	C(7)−Ir(2)−Cl(1)	98.3(10)	N(1)−Ir(1)−I	91.3(4)		
N(1)−Ir(1)−C(1)	94.7(12)	N(2)−Ir(2)−P(2)	104.2(6)	N(1)−Ir(1)−Cl(2)	87.9(8)	N(2)−Ir(2)−P(2)	103.7(4)		
N(4)−Ir(2)−C(2)	98.(3)	C(8)−Ir(1)−N(1)	89.6(11)	N(4)−Ir(2)−Cl(1)	88.1(7)	C(8)−Ir(1)−N(1)	89.4(7)		
		C(7)−Ir(2)−N(2)	94.7(10)	N(3)−Ir(1)−Cl(2)	90.0(8)	C(7)−Ir(2)−N(2)	91.8(8)		
		P(1)−Ir(1)−Ir(2)	100.3(2)	N(2)−Ir(2)−Cl(1)	89.0(7)	P(1)−Ir(1)−Ir(2)	99.5(1)		
		P(1)−Ir(1)−N(4)	90.4(6)	N(1)−Ir(1)−Ir(2)	69.5(7)	P(1)−Ir(1)−N(4)	89.5(4)		
		P(1)−Ir(1)−Cl	93.4(3)	N(4)−Ir(2)−Ir(1)	70.3(6)	P(1)−Ir(1)−I	95.2(1)		
		P(1)−Ir(1)−C(8)	96.3(9)	N(3)−Ir(1)−Ir(2)	69.7(8)	P(1)−Ir(1)−C(8)	97.5(6)		
				N(2)−Ir(2)−Ir(1)	69.7(7)				
				P(2)−Ir(1)−Ir(2)	111.0(2)				
				P(1)−Ir(2)−Ir(1)	110.4(2)				
				C(8)−Ir(1)−Ir(2)	102.1(11)				
				C(7)−Ir(2)−Ir(1)	103.7(10)				

[a] These two distances were influenced by a constraint in the refinement.

occupation by H (i.e., trans, **2**, or cis[8]) is at conspicuous variance with the axial entry of addenda that is followed in the more typical oxidative pathway, where nucleophilic (S_N2-like) behavior of the bimetallic center is recognizable.[3−5,9] That the structure of the thermodynamic product of this type of dihydrogen addition says nothing about the mechanism by which it is formed has been amply demonstrated in a very interesting reinvestigation of corresponding diiridium "A-frame" chemistry by Eisenberg and co-workers.[14] The related but reversible reaction of a novel mixed-valence bis(bis(trifluoroethoxy)phosphino)methylamine-bridged Ir^0-Ir^{II} (d^9-d^7) dimer with H_2 affords a Ir^I-Ir^{III} dihydride (d^8-d^6) in which Ir−Ir = 2.7775(11) Å. In this product, the two hydrogen atoms (not located) that are attached to different iridium centers are found[13] at sites that are distal (i.e., like those in **2**) rather than proximal (i.e., cis[8]).

The binuclear dihydride **2** reacts in boiling carbon tetrachloride with replacement of one (but not both) H by Cl, affording compound **3** (Scheme 1). Under the same conditions, **1** undergoes two-center oxidative addition to give the 1,2-dichloro adduct **4** (the 4-chloro-pyrazolyl-bridged analogue of which is formed[15] by dichlorine addition to **1**). Oxidation of **1** using diiodine yields an analogue [IrI(μ-pz)(PPh$_3$)(CO)]$_2$ (**5**) of **4**, which reacts with tetrahydroaluminate ion to replace one (but not both) I by H, affording the homologue **6** of **3**. While the X-ray structure of **4** is unremarkable (molecular C_2 symmetry; see Figure 2, which shows the axial disposition of each Cl and where the Ir−Ir bond distance is 2.754 Å), those of **3** and **6** (which are isomorphous) are consistent with the idea that the accommodation of the trans influences exerted by Ir−Ir and Ir−H bonds is a primary factor in determining the equilibrium geometry. Thus, in each molecule, as is shown in Figures 3 and 4, the (single) hydride is equatorial (detected as an obvious vacancy), and the phosphine ligand that is attached to the same Ir center is oriented axially. By contrast, at the second Ir site, the phosphine and halide occupy positions (equatorial and axial, respectively) corresponding to those

(23) Thorez, A.; Maisonnat, A.; Poilblanc, R. *Inorg. Chim. Acta* **1977**, *25*, L19.

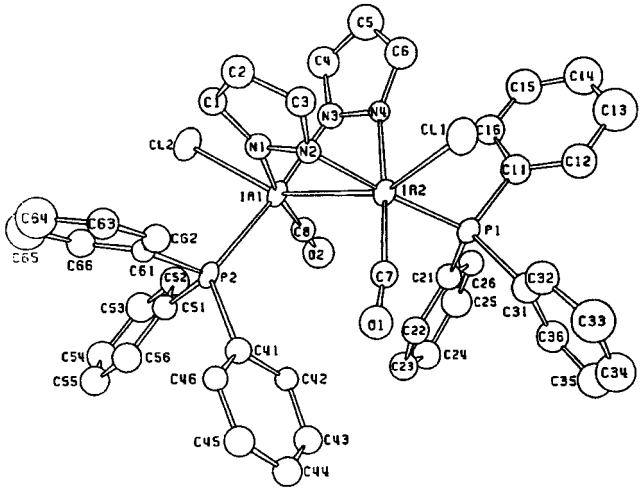

Figure 2. Molecular geometry of compound **4**.

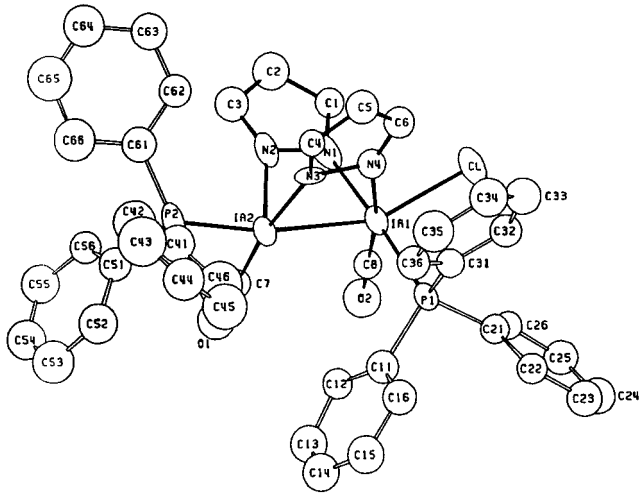

Figure 3. Molecular geometry of compound **3**.

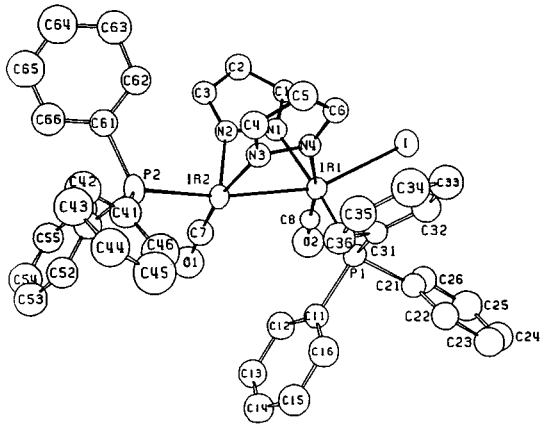

Figure 4. Molecular geometry of compound **6**.

in compound **4** (see Table 3). The resistance of these diiridium(II) adducts to reductive elimination (i.e., of HX for **3** and **6**, X = Cl or I, respectively) is underscored by the independent observation that dimer **1** is quantitatively cleaved to mononuclear species[22] using HX (X = Cl, Br, or I) as reagents.

The reaction of **1** with fluoroboric acid affords a chrome-yellow product, **7**, having a structure in solution that is

Scheme 3

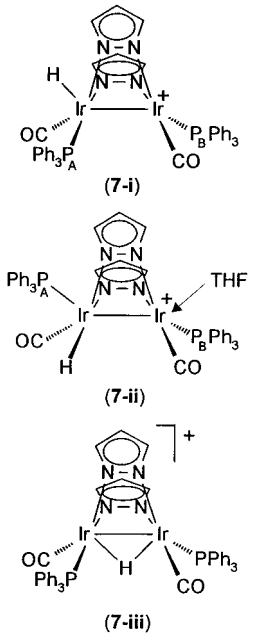

unambiguously recognizable on the basis of temperature-invariant ^{1}H and ^{31}P NMR data as an unsymmetrically substituted, binuclear species with a single hydrogen atom bound to only one metal center (i.e., it shows two distinguishable environments for μ-pz 3-, 4-, and 5-hydrogens and for P nuclei). Protonation (by HBF_4 or HO_3SCF_3) of a diamidonaphthalene-bridged diiridium(I) complex that is a direct analogue of **1** has been described very recently by Oro and co-workers.[24] The cation so obtained, which displays NMR parameters that are almost identical to those of **7** and was likewise concluded to contain a hydride ligand bound terminally at one Ir atom, undergoes a sequence of chemical changes that lend convincing support to such a formulation. Further consideration of data from the same source indicates[24] that if terminal H at Ir occupies an axial site, a ^{1}H resonance is observed as a doublet of doublets (i.e., through coupling to a distant P_B, across the Ir−Ir bond, as well as to an adjacent (cis, P_A) phosphorus nucleus). By contrast, equatorial disposition allows only cis coupling (to P_A) to be resolved, and the pattern simplifies to a doublet. We believe that this accounts for the difference in the NMR spectra of **7**/CH_2Cl_2 and **7**/THF, with the donor capacity of THF leading to the solvation of vacant axial sites in **7**, which destabilizes axial hydride coordination (see Scheme 3, **7-ii** versus **7-i**).

The earlier data also suggest[24,25] that there is a delicate energetic balance between terminal- and bridging-hydride geometries. It is perhaps not surprising, therefore, that upon crystallization the binuclear cations of **7** are ordered into a rigorous two-fold relationship, with each BF_4^- counterion in a position that, while distant, is centered on the same C_2

(24) Jiménez, M. V.; Sola, E.; López, J. A.; Lahoz, F. J.; Oro, L. A. *Chem.—Eur. J.* **1998**, *4*, 1398. See also Oro, L. A.; Sola, E.; López, J. A.; Torres, F.; Elduque, A.; Lahoz, F. J. *Inorg. Chem. Commun.* **1998**, *1*, 64. Torres, F.; Sola, E.; Elduque, A.; Martinez, A. P.; Lahoz, F. J.; Oro, L. A. *Chem.—Eur. J.* **2000**, *6*, 2120.

(25) Sola, E.; Bakhmutov, V. I.; Torres, F.; Elduque, A.; López, J. A.; Lahoz, F. J.; Werner, H.; Oro, L. A. *Organometallics* **1998**, *17*, 683.

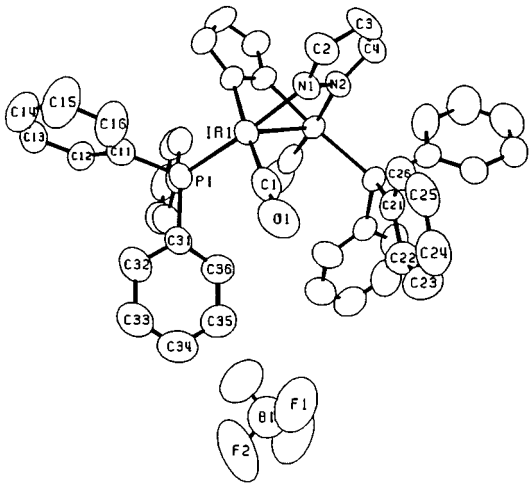

Figure 5. Molecular geometry of compound **7**.

axis. The resulting arrangement is shown in Figure 5 (50% thermal ellipsoids are larger for the isolated tetrahedral anion, as is typical for such units). The bridging hydrogen was not found, possibly because of thermal motion that may represent positional averaging of an atom that is unsymmetrically[24] bonded between the metal nuclei, but the remaining hydrogens were all successfully included in the refinement. This showed that an ortho H of a Ph substituent at P (i.e., H attached to C-16, Figure 5) is placed close enough to Ir (i.e., 3.06 Å), by rotation of the phosphine ligand, to rule out the occupancy of an exo (axial) site by a terminal hydride. Occupation of a terminal site by hydride would therefore necessarily lead to a H···H approach ≤1.75 Å. The cation configuration is superficially identical to that of the neutral prototype **1**, but the Ir_2 distance is contracted from 3.163 to 2.834 Å (i.e., into bonding range), although it is evidently somewhat longer than those in **2**−**4** and **6** (Table 3). This observation is also consistent with the presence of a bridging-hydride interaction. The solid-state, hydride-bridged, metal−metal-bonded representation for **7** (Scheme 3, **7-iii**) clearly corresponds to a $d^7{}_2$ diiridium(II) formalism, in contrast to the solution structure (**7-i** or **7-ii**), which might equally well be viewed[24] as d^6d^8 (i.e., $Ir^{III}Ir^{I}$).

The reactivity of **7** in ostensibly dry solvents provided the first clue to the sensitivity of the complex to hydrolysis. Subsequent experiments led to the isolation of another cation, **8**, identified as a symmetrical binuclear species on the basis of its NMR properties. Observation of a doublet signal at −17.95 ppm in the ^{1}H NMR spectrum that is attributable to a terminal hydride, the relative intensity of which is reduced by half when ^2H_2O is used as a reactant instead of water, together with two ^{31}P resonances that are resolved (−140.28, −140.37 ppm) from one another, are consistent with formation of the isotopomer $[Ir_2(H)(^2H)(\mu\text{-pz})_2(\mu\text{-}O^2H)(PPh_3)_2(CO)_2]BF_4$. This reaction was observed to be complete, with no side products formed, after 10 d in a solution containing only 5 ppm H_2O. It is not possible to distinguish axial (exo) hydride attachment from equatorial hydride attachment (see Scheme 2) on the basis of these data, although the thermodynamic preference in related chemistry appears to be axial.[24] A parallel reaction in wet methanol yielded an approximate 30:70 mixture of **8**/**9**, in which **8** is the minor product and **9** (Scheme 2) is a symmetrical analogue of **8**. These results, when taken with the fact that **1** is unaffected by water or methanol, imply that the products are formed by nucleophilic attack on the cation of **7**. There are very few other examples of discrete transition-metal (hydroxo)hydrido complexes, and none of them have been synthesized in a similar manner.[19]

Reaction of **1** with trifluoroacetic acid afforded a neutral complex, rather than a cationic product like **7**, that was shown by mass spectrometry to be dimeric, although it was not obtained as crystalline material. While the cations of **8**−**11** are expected, by comparison with related species,[6,17,22] to adopt a bioctahedral arrangement that is triply bridged, consideration of the stoichiometry and spectroscopic properties of the **12** are indicative of a more open structure in which the octahedra containing the adjacent d^6 Ir(III) centers are likely to be connected only through the pyrazolyl-bridged framework (see Scheme 2).

Acknowledgment. We thank the N.S.E.R.C., Canada, for financial support, Dr. R. Vefghi for conducting certain exploratory experiments, and Mrs. K. Beveridge for technical assistance with crystallography.

Supporting Information Available: Full crystallographic details including tables of fractional atomic coordinates, anisotropic temperature factors, interatomic distances, and bond angles for compounds **2**−**4**, **6**, and **7**. This material is available free of charge via the Internet at http://pubs.acs.org.

IC010448G